Received: 07 July 2023, Accepted: 15 August 2023

Original Research

Journal of Advanced Veterinary Research
(2023) Volume 13, Issue 8, 1566-1574

Nephroprotective Effect of N-Acetyl-L-Cysteine against Diazinon-induced Nephrotoxicity in Rats via IKβ, NFκB, NLRP3 Signaling Pathway

Eman M. Fath[1], Hatem H. Bakery[1], Ragab M. EL-Shawarby[1], Mohamed E.S. Abosalem[1], Nesrine Ebrahim[2,3,4], Ahmed Medhat Hegazy[1*], Samer S. Ibrahim[1]

[1]Department of Forensic Medicine and Toxicology, Faculty of Veterinary Medicine, Benha University, Moshtohor, Toukh 13736, Qalyubia, Egypt.

[2]Department of Histology and Cell Biology Faculty of Medicine, Benha University, Benha 13511, Egypt.

[3]Stem Cell Unit, Faculty of Medicine, Benha University, Benha 13511, Egypt.

[4]Benha National University, Faculty of Medicine, Obour City, Egypt.

***Correspondence**
Corresponding author: Ahmed Medhat Hegazy
E-mail address: ahmed.hegazy@fvtm.bu.edu.eg

Abstract

The present study analyzes the efficacy of N-acetyl cysteine (NAC) against diazinon (DZN)-induced nephrotoxicity in male Wistar rats. Rats were divided into five groups with six animals in each group: Group 1 (G1) was maintained in typical control circumstances and given saline once daily intragastric (IG) for 4 weeks; G2 was administered 0.1 mL olive oil IG for 4 weeks; G3 was administered IG NAC 150 mg/kg daily as an aqueous solution for 4 weeks; G4 was administered IG diazinon at a dose of 15 mg/kg daily for 4 weeks; and G5 was administered IG NAC daily one hour before diazinon at the same dose in G3 and G4 for 4 weeks. Sub-chronic exposure to DZN impairs the kidney structure and function, as evidenced by the histopathology, immunohistochemistry, and gene expression of NLRP3, NFκB, IKB, BCL2, BAX mRNA. Our findings showed that NAC reduces the renal dysfunctions induced by DZN by restoring urea and creatinine levels as well as oxidative indicators. Moreover, serum inflammatory markers (IL-1β and TNF-α) concentrations were ameliorated by NAC treatment. However, NAC has shown to play a beneficial role against nephrotoxicity by reversing the cytoarchitecture and downregulation of inflammatory (NLRP3, NFκB, IKB) and apoptotic (BAX) as well as upregulated BCL2 genes and proteins in kidney tissues, bringing them to near-normal levels. Moreover, IHC examination of renal tissue revealed the attenuation of expression of TNF-α. Therefore, NAC could be potentially used to protect the kidneys from pathological changes induced by DZN.

KEYWORDS
Diazinon, N-acetyl cysteine, Nephrotoxicity, NLRP3, Oxidative stress.

INTRODUCTION

Insecticides comprise a higher proportion of the total pesticide usage in developing countries than in developed countries. Organochlorine (OC), organophosphorus (OP), carbamate, pyrethroid, and different inorganic compounds are the main groups that have been utilized as insecticides (Eddleston *et al*., 2002). Residual amounts of OP and OC pesticides have been detected in soil, water bodies, vegetables, grains, and other foods products (Pathak *et al*., 2022). Organophosphate insecticides are a group of insecticides acting on the enzyme acetylcholinesterase. They disrupt this enzyme in a variety of ways, rendering it permanently inactive and increasing the risk of poisoning in both humans and many other creatures, including insects. This enzyme is crucial for nerve activity (Hamad *et al*., 2016).

In recent years, agricultural use of the organophosphate insecticide diazinon (DZN), [O, O-diethyl-O-(2-isopropyl-4-methyl-6-pyrimidinyl) phosphorothionate], has increased significantly. DZN can cause biochemical, physiological, and histological changes in several organs, including the liver, kidney, heart, testis, and brain, according to several investigations in rabbits, rats, and mice (Smith *et al*., 2018). These harmful effects have been linked to oxidative stress, DNA damage, and pro-inflammatory activities that increase reactive oxygen species generation and decrease antioxidant enzyme activity (Danaei *et al*., 2019).

N-acetyl cysteine (NAC), a well-known antioxidant, has been demonstrated to be a potent disulphide linkages disruptor (Aldini *et al*., 2018). NAC is a safe and affordable medication, that is accessible as an over-the-counter supplementation (Mokhtari *et al*., 2017). The metabolism of NAC to L-cysteine, a precursor to glutathione, increases glutathione-S-transferase activity. As a result, NAC boosts the concentration of free glutathione in cells, supports detoxification, and guards against the damaging effects of various free radical species (Owumi *et al*., 2021).

NAC's pharmacological effects include the reduction of neutrophil activity and the generation of TNF, as well as the restoration of cellular antioxidant potential by refilling glutathione that has been depleted by free radicals and ROS (Joshi *et al*., 2014).

N-acetylcysteine is the acetylated variant of the amino acid L-cysteine and is widely used as the specific antidote for acetaminophen overdose. The prevention of chronic obstructive pulmonary disease exacerbation, the avoidance of contrast-induced kidney injury during imaging procedures, the treatment of pulmonary fibrosis, and the treatment of infertility in patients with clomiphene-resistant polycystic ovary syndrome are additional uses for N-acetylcysteine supplementation that are supported by scientific evidence. N-acetylcysteine may also play a role in the prevention of cancer, as an adjuvant in the treatment of Helicobacter pylori, and in the prevention of gentamicin-induced hearing loss in patients receiving renal dialysis, according to pre-

ISSN: 2090-6277/2090-6269/

liminary investigations (Millea, 2009).

However, to the best of our knowledge, there are currently no available studies that investigate the effects of NAC against diazinon-induced kidney damage. As such, the aim of this study was to investigate the possible beneficial effects of NAC regarding its prevention of oxidative stress and inflammatory pathways induced renal damage in rats.

MATERIALS AND METHODS

Ethical approval

Regulations set forth by the Institutional Animal Ethics Committee were followed when conducting the current investigation, as well as Approval Protocol Number: BUFVTM 04-04-21 from Benha University in Egypt.

Chemicals

N-acetylcysteine (NAC) were purchased from Aldrich Company, USA. Diazinon (DZN) was purchased from High Control Company in Naser City, Cairo, Egypt.

Experimental animals

Twelve weeks old male adult Wistar rats (weighing 200 to 250 g) were purchased from the Faculty of Veterinary Medicine, Experimental Animal Unit, Benha University, Egypt. Rats were housed in orderly cages and were provided with clean food and water on demand. All rats were kept in standard conditions, including a room temperature of 23°C, a 12-hour light/dark cycle, and free water and food were available. Prior to therapy, baseline body weight measurements were performed for all groups. Weekly animal weights were taken in order to modify the chemical dosage.

Experimental design

Five equal groups of six adult male Wistar rats each were created from a total of 30 rats. The initial group (G1) was kept as a healthy control and given 0.1 mL intragastric saline once daily for 4 weeks. The second group (G2) was administered 0.1 mL olive oil once daily for 4 weeks. The third group (G3) was administered intragastric NAC at a dose of 150 mg/kg b.wt. daily for 4 weeks (Oksay *et al*., 2013). The fourth group (G4) was administered intragastric DZN (dissolved in olive oil) intragastric at a dose of 15 mg/kg b.wt. daily for 4 weeks (Rashedinia *et al*., 2016). The fifth group (G5) was administered intragastric NAC daily one hour before DZN at the same dose in G3 and G4 daily for 4 weeks. The experimental rats were euthanized with isoflurane after the study was completed before being killed by decapitation, then blood samples were collected from the heart for estimation of the urea and creatinine. Tissue samples were collected for estimation of the interleukins [Interleukin-1 beta (IL-1β) and Tumor necrosis factor alpha (TNF-α)], oxidative markers [catalase (CAT), superoxide dismutase (SOD), glutathione peroxidase (GPx), reduced glutathione (GSH) and malondialdehyde (MDA)], gene expression [IKβ, NFκB, NLRP3, BCL2, BAX mRNA genes], the preservation of tissue samples were at -80oC prior to analysis. Part from the kidney tissue was used for histopathological examination.

Preparation of kidney homogenate

According to Hegazy *et al*. (2020), kidney tissue homogenates were prepared. The oxidative indicators [catalase activity (CAT), superoxide dismutase activity (SOD), quantity of glutathione peroxidase (GSH-Px), quantity of reduced glutathione (GSH), and lipid peroxidation by-products malondialdehyde (MDA)], and total protein were measured in the collected supernatant.

Assay methods

Kidney function tests

Serum urea and creatinine concentrations were measured by Bio-Diagnostic commercially available kits following the method of Skeggs (1957) and Weissman *et al*. (1974); respectively.

Oxidative markers in kidney tissue homogenate

According to using commercially available ELISA kits (Biovision Inc. 155S Milpitas Blvd, Milpitas, CA, 95035 USA); catalase (CAT), superoxide dismutase (SOD), glutathione peroxidase (GSH-Px), reduced glutathione (GSH) and malondialdehyde (MDA) were determined colorimetrically. Based on Bradford (1976) method, the tissue homogenate's protein content was measured using Genei, Bangalore protein estimation kit. An Enzyme-Linked Immuno-Sorbent Assay (ELISA) plate reader (Stat Fax 2200, Awareness Technologies, Florida, USA) was used to measure color absorbance.

Cytokines in kidney tissue homogenate

Interleukin-1 beta (IL-1β) and Tumor necrosis factor alpha (TNF-α) were determined in kidney tissue homogenate using commercially available ELISA kits (Cloud-Clone Corp Co., Houston, USA) in line with the instructions provided by the manufacturer.

Kidney mRNA gene expression

Real-time polymerase chain reaction (PCR) was used to assess the mRNA gene expression of the kidney's IKβ, NFκB, NLRP3, BCL2, BAX genes. At end of fourth-week rat's kidney specimens were quickly removed and weighed, then washed with cold saline to exclude the blood cells and then blotted on filter paper; it was kept in RNAlater storage reagent for gene expression at -80ºC. Total RNA was extracted from kidney tissues using TRIzol (Invitrogen) according to the manufacturer's instructions. The concentration and purity of extracted RNA were measured by Nano Drop 2000C spectrophotometer (Thermo Scientific, USA). At absorbance ratio A260/A280, RNA purity for all samples was > 1.9. The integrity of RNA was verified on 2% agarose gel using gel electrophoresis image (Gel Doc. BioRad). Complementary DNA (cDNA) were synthesized for the target genes using SensiFast cDNA synthesis kits (Sigma Bioline, UK) according to the manufacturer's instruction. NCode VILO miRNA cDNA Synthesis Kit (Invitrogen) were used for cDNA Synthesis from miRNAs following the manufacturer's recommendations. SuperScript IV One-Step RT-PCR kit (Cat# 12594100, Thermo Fisher Scientific, Waltham, MA USA) was utilized for reverse transcription of extracted RNA followed by PCR in one step as shown in table 1. Each sample was performed in triplicate and the non-template control (NTC) was run also to test the presence of primer-dimer and cDNA contamination. The expressions of renal IKβ, NFκB, NLRP3, BCL2, BAX, and GAPDH were analyzed by real time PCR using sense and anti-sense primers throughout the experiment using the primers sets in Table 2. Thermal cycling and fluorescence detection were performed using a 7300 real-time-PCR system (Applied Biosys-

tems, Foster City, CA, USA) using conditioned showed in Table 3. Cycle threshold (Ct) values acquired from real-time PCR equipment were applied to a reference (housekeeping) gene (GAPDH) to detect changes in gene expression (Livak and Schmittgen, 2001).

Table 1. SuperScript™ IV One-Step RT-PCR with ROX components:

Component	Reaction (1X)
SuperScript™ IV RT Mix	0.5 µl
2X Platinum™ SuperFi™ RT-PCR Master Mix	25 µL
Forward primer (10 µM)	2.5 µL
Reverse primer (10 µM)	2.5 µL
Template RNA	10 µl
Nuclease free water	9.5 µl
Final Volume	50 µl

Protein markers in kidney tissue homogenate

We used the Bio-Rad Inc. ReadyPrepTM protein extraction kit (Catalogue #163-2086) for kidney tissue proteins extraction. Protein concentrations were measured using the Bradford Protein Assay Kit (SK3041) from Bio Basic INC (Markham, Ontario, L3R 8T4 Canada). The loading quantity of protein samples were 20µg. The extracts were separated by Sodium Dodecyl Sulfate Polyacrylamide Gel Electrophoresis (SDS-PAGE) (12%), and then transferred to poly-vinylidene fluoride (PVDF) membrane (7min at 25V). After blocking the membrane for an hour at room temperature with tris-buffered saline with Tween 20 (TBST) buffer and 3% bovine serum albumin (BSA), the membrane was subjected to a variety of primary antibodies. Primary antibodies of NLRP3, NFκB, IKB, BCL2, BAX, and β-actin were purchased from OriGene Technologies Inc (9620 Medical Center Drive, Ste 200 Rockville, MD 20850, USA). Then the primary antibodies were treated at 4oC overnight as anti-NLRP3, anti-NFκB, anti-IKB, anti-BCL2, anti-BAX, and anti-β actin (housekeeping protein). For five minutes, the blot was being rinsed with TBST 3-5 times. The goat anti-rabbit IgG- HRP-1 mg Goat mab- Novus Biologicals secondary antibody solution was treated with the target protein for 1 hour at room temperature. The blot was then rinsed with TBST three times for five minutes. The blot was covered with the chemiluminescent substrate (Catalogue no. 170-5060, ClarityTM Western ECL substrate Bio-Rad). The chemiluminescent signals were captured using an imager that is based on a CCD camera. By protein normalization on the ChemiDoc MP imager, band intensity of the target proteins was read against the control sample β-actin (housekeeping protein).

Histopathological examination

All groups had kidney samples collected right away, which were then fixed for 24 hours in 10% buffered neutral formalin. Following convenient fixing, the samples were cleaned in xylol, embedded in paraffin, dehydrated in various grades of ethyl alcohol, blocked, and sectioned into 4 µm thick sections. Followed by hematoxylin and eosin, and Masson's trichrome staining and microscopic examination (Suvarna *et al*., 2019).

Immunohistochemical study

Deparaffinized and hydrated paraffin sections were used. The sections were first blocked for non-specific reactions with 10% hydrogen peroxide, followed by incubation with primary rabbit polyclonal antibodies against TNF-α [TNFA/1172] (ab220210); a concentration of 2-4 µg/ml was used. Perform heat mediated antigen retrieval with citrate buffer pH 6 before commencing with IHC staining protocol, abcam, UK). and rabbit polyclonal to SERCA2 ATPase (ab3625, a concentration of 1 µg/ml was used. Perform heat mediated antigen retrieval before commencing with IHC staining protocol, abcam , UK). Before beginning with IHC staining technique (Abcam, UK) and rabbit polyclonal to SERCA2 ATPase (ab3625, a concentration of 1 g/ml was used), heat-mediated antigen retrieval with citrate buffer pH 6 was done. Before beginning the IHC staining process, heat-mediated antigen retrieval (Abcam, UK) was perfomed. Next, a biotinylated goat anti-rabbit secondary antibody was used after phosphate buffer washed the cells. To localize the immunological response, the slides were treated with labelled avidin-biotin peroxidase, which binds to the biotin on the secondary antibody. For visualizing the location where an antibody binds and peroxidase transforms it into a brown precipitate, diaminobenzidine was used as a chromogen (Suvarna *et al*., 2013).

Table 2. The evaluated genes' primer sets.

Gene symbol	Forward	Reverse	Gene bank
IKβ	CTGTGCACGTCATTTGTGGG	CAGTTAGGGAGAAAGGGCCG	NM_053355.2
NFκB	TCTGTTTCCCCTCATCTTTCC	GCGTCTTAGTGGTATCTGTGCTT	AF079314.2
NLRP3	GTAGGTGTGGAAGCAGGACT	CTTGCTGACTGAGGACCTGA	XR_005489722.1
BAX	CGGCGAATTGGAGATGAACTGG	CTAGCAAAGTAGAAGAGGGCAACC	XM_032915032.1
BCL2	TGTGGATGACTGACTACCTGAACC	CAGCCAGGAGAAATCAAACAGAGG	XR_005492200.1
GAPDH	CACCCTGTTGCTGTAGCCATATTC	ACATCAAGAAGGTGGTGAAGCAG	XM_032910454.1

Table 3. The Thermal profile cycling of RT-qPCR.

Step		Cycle	Temp.	Time
Reverse Transcription (RT)		1	55°C	10 mins
RT Enzyme inactivation		1	95°C	2 mins
Amplification	Denaturation	40	95°C	10 secs
	Annealing		55°C	10 secs
	Extension		72°C	30 secs
Final extension		1	72°C	5 mins

Morphometric study

Using the Image-Pro Plus programme version 6.0 (Media Cybernetics Inc., Bethesda, Maryland, USA), the mean area percentage of collagen fiber deposition, TNF-α immuno-expression were calculated. The mean area percentage was determined for five photographs taken from five different fields for each rat in each group.

Statistical analysis

The statistical analysis was completed using the SPSS for Windows (Version 18.0; SPSS Inc., Chicago, Illinois) statistical software for social research. With Duncan's post hoc analysis, the one-way ANOVA test was utilized to identify significant differences between experimental groups. The mean and standard error of the mean (SEM) are used to express results. A P-values lower than 0.05 were regarded as significant.

RESULTS

Throughout the study period, there were no deaths reported among the various treatment groups.

Serum urea and creatinine

Table 4 displays the mean and standard errors of the various groups' serum urea and creatinine levels. Urea and creatinine levels were increased noticeably in G4 (rats treated with DZN) compared to normal control, olive oil, and NAC treated groups after 4 weeks of the experiment. However, rats co-treated with both NAC and DZN (G5) had significantly lower serum urea and creatinine levels than the DZN treated group.

Changes in the kidney oxidative markers

Table 5 shows the mean and standard errors of the individual groups' oxidative markers. Rats in G4 treated with DZN had significantly higher levels of MDA in the kidney tissue than the healthy control, olive oil, and NAC treated groups. While treatment of rats with both DZN and NAC (G5) showed significant decreases in MDA level when compared with the toxic group after 4 weeks of the experiment. Likewise, the values of CAT, SOD, GPx, and GSH in the kidney tissue of the toxic rats (G4) treated with DZN showed markedly decreased than the normal control, olive oil, and NAC treated groups. However, treatment of the toxic rats with NAC (G5) resulted in a considerable rise in the CAT, SOD, GPx, and GSH level when compared with the toxic group (G4) after 4 weeks of the experiment.

Changes in kidney cytokines

As displayed in Figure 1; the rats (G4) that were treated with DZN showed increased levels of serum concentrations of IL-1β and TNF-α compared to normal control, olive oil, and NAC treated groups after 4 weeks of the experiment. However, rats co-treated with both NAC and DZN (G5) had significantly lower serum concentrations of IL-1β and TNF-α levels than toxic group (G4).

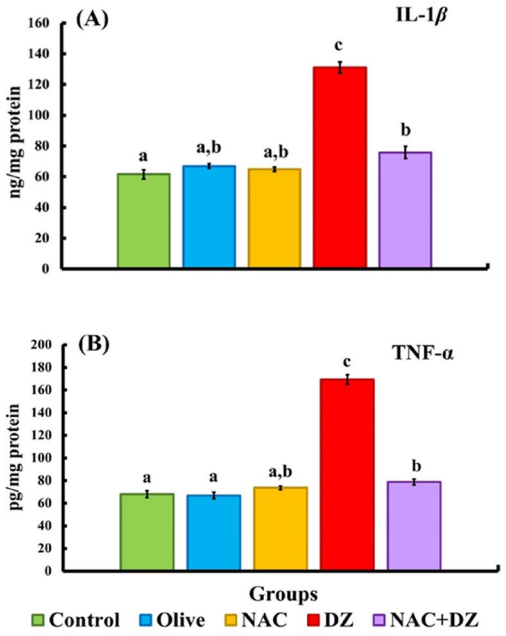

Fig. 1. Effect of N-Acetyl-Cysteine (NAC) versus diazinon (DZN) on IL-1β and TNF-α levels of various study groups after 4 weeks of treatment The bars show the mean and standard error (n=6).

IKβ, NFκB, NLRP3, BCL2, and BAX mRNA expression in kidney tissue

As displayed in Figure 2, the expression of kidney IKβ, NFκB, NLRP3, BCL2, and BAX mRNA genes in the control, olive oil, NAC,

Table 4. Effect of N-Acetyl-Cysteine (NAC) versus diazinon (DZN) on serum urea and creatinine levels in various study groups after 4 weeks of treatment, (n=6).

	Control	Olive	NAC	DZN	NAC+DZN
Urea (mg/dL)	27.31±1.09^{a}	22.64±1.29^{a}	30.47±1.34^{a}	89.48±4.42^{c}	70.55±3.34^{b}
Creatinine (mg/dL)	0.70±0.03^{a}	0.59±0.02^{a}	0.73±0.02^{a}	4.63±0.27^{c}	3.24±0.35^{b}

Data are expressed as mean±standard error. Means with different superscripts in the same row are significantly different at p<0.05.

Table 5. Effect of N-Acetyl-Cysteine (NAC) versus diazinon (DZN) on oxidative markers in the kidney homogenates of various study groups after 4 weeks of treatment, (n=6).

	Control	Olive	NAC	DZN	NAC+DZN
CAT (U/mg protein)	2.67±0.28^{b}	2.84±0.48^{b}	2.50±0.28^{b}	1.10±0.08^{a}	2.80±0.25^{b}
SOD (U/mg protein)	2.90±0.18^{b}	3.12±0.41^{b}	2.80±0.16^{b}	1.09±0.09^{a}	2.60±0.10^{b}
GPx (nmol/mg protein)	25.22±1.79^{c,d}	28.54±3.36^{d}	22.40±1.03^{b,c}	10.30±0.74^{a}	20.38±0.88^{b}
GSH (µg/mg protein)	1.60±0.11^{b}	1.62±0.16^{b}	1.41±0.06^{b}	0.66±0.08^{a}	1.44±0.04^{b}
MDA (nmol/mg protein)	0.51±0.06^{a}	0.50±0.06^{a}	0.56±0.07^{a}	2.60±0.37^{b}	0.72±0.00^{a}

Data are expressed as mean±standard error. Means with different superscripts in the same row are significantly different at p<0.05.

DZN, and NAC-DZN-treated groups after 4 weeks of treatment. The intoxicated rats induced a marked upregulation in kidney IKβ, NFκB, NLRP3, and BAX mRNA with a marked downregulation in kidney BCL2 mRNA. However, treatment of intoxicated rats with NAC induced a marked downregulation of IKβ, NFκB, NLRP3, and BAX mRNA genes with a marked upregulation in kidney BCL2 mRNA.

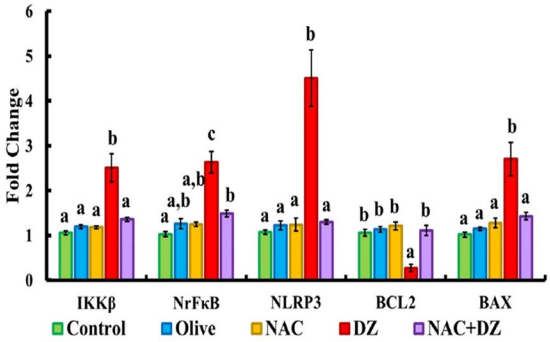

Fig. 2. mRNA expression of IKKβ, NFκB, NLRP3, BCL2, and BAX in the kidney's mRNA. Four weeks following treatments, total RNA was extracted from the kidney tissues of rats given olive oil, N-Acetyl-Cysteine (NAC), diazinon, NAC vs diazinon, and control. Real-time PCR was used to assess expression levels, with a p-value<0.05 when compared to control values. The bars show the mean and standard error (n=6).

Changes in kidney protein markers

As displayed in Figure 3, the average relative density of kidney NLRP3, NFκB, IKB, BAX, and BCL2 normalized to β-actin in the NAC, DZN, and NAC-DZN-treated groups than normal control and olive oil treated groups after 4 weeks of experiment. Comparing the intoxicated group (G4) to the healthy control and olive oil groups, revealed noticeably higher level of NLRP3, NFκB, IKB, and BAX as well as a substantial drop in BCL2 protein markers in kidney tissue. After 4 weeks of the experiment, the intoxicated group that had received NAC treatment (G5) had significantly lower level of NLRP3, NFκB, IKB, and BAX as well as significantly higher levels of BCL2 compared to the intoxicated group (G4).

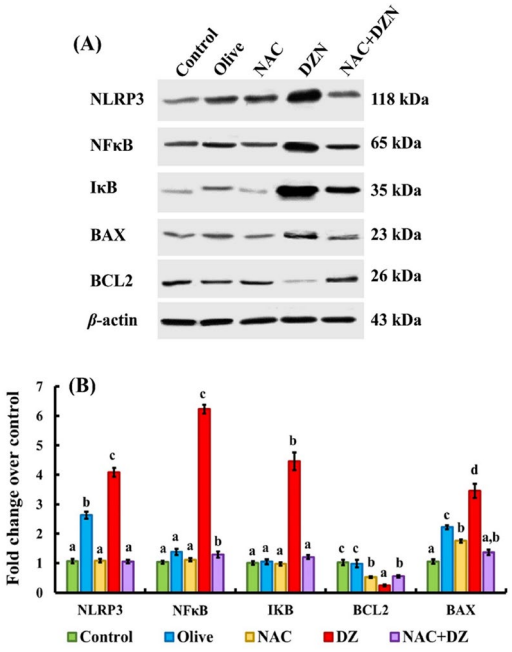

Fig. 3. Western blotting with densitometric analysis of NLRP3, NFκB, IKB, BAX, and BCL2 proteins in kidney tissue of rats treated with olive oil, N-Acetyl-Cysteine (NAC), diazinon, NAC versus diazinon, and control on 4 weeks after treatments (n=6).

Histopathological assessment of kidney tissue

Examination of kidney sections revealed that intoxicated rats (G4) showed dilated Bowman's space, inflammatory cell infiltration, glomerular and peritubular vascular congestion and swelling of renal tubular epithelium cells (Figure 4d). Co-treatment of intoxicated rats with NAC showed nearly normal histological structure as there were decreased of Bowman's space dilatation, inflammatory cell infiltration, reduction of glomerular and peritubular vascular congestion and reduction of the renal tubular epithelium cells swelling (Figure 4E). The kidney tissues of rats that administered olive oil, NAC as well as the normal control group appeared to be normal; they revealed renal corpuscles consisting of glomeruli surrounded by narrow Bowman's space and Bowman's capsule. The corpuscles were surrounded by proximal and distal convoluted tubules (Figure 4A, B, and C).

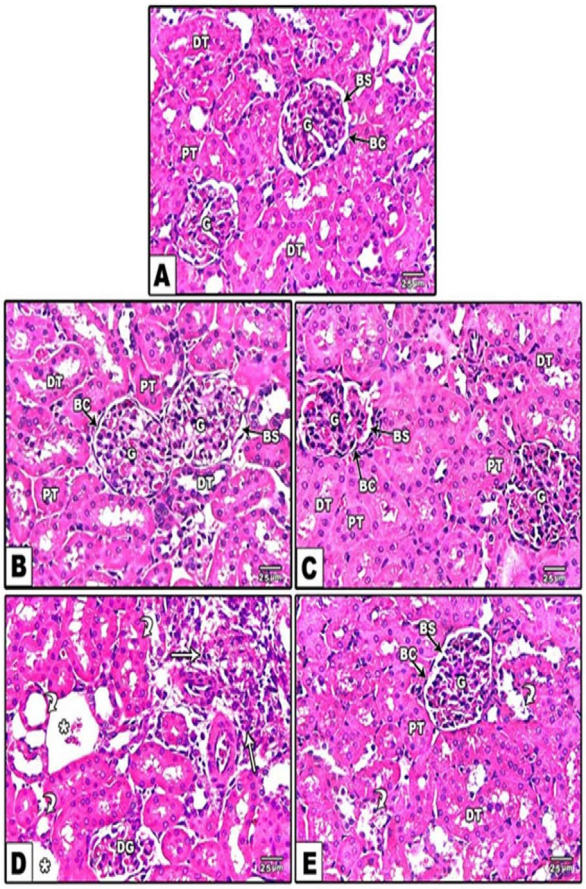

Fig. 4. Photomicrograph from kidney of experimental rats. (A), (B), and (C) Normal control rat (G1), Olive oil treated rats (G2) and rat treated with N-Acetyl-Cysteine (NAC) (G3), the kidney showed normal glomerulus (G) and Bowmen's capsule, distal tubule tubules (DT) and proximal tubules (PT). (D) Intoxicated rats (G4) induced by diazinon; showed dilatation of Bowman's space and degenerated glomeruli (DG) and inflammatory cell infiltration (arrow); glomerular and peritubular vascular congestion, swelling of renal tubular epithelium cells (curved arrow). (E) Intoxicated rat by diazinon then treated with NAC (G5), showed normal glomeruli (G) and tubules (PT andDT). (HandE,×200) (Scale bar represents 25 μm).

Masson's trichrome stain examination

Examination of kidney sections stained with Masson's trichrome showed that the intoxicated group (G4) displayed a significant increase in the amount of collagen fiber deposition between the tubules and among the glomerular capillaries (Figure 5D). On the other hand, the intoxicated group treated with NAC (G5) showed decreased amounts of collagen fibers among the glomerular capillaries and surrounding the renal corpuscles

and tubules (Figure 5E). The minimal amounts of collagen fibers among the glomerular capillaries and surrounding the renal corpuscles and tubules were detected in the normal control, olive oil, and NAC-treated groups (Figure 5A, B, and C).

Immunohistochemical assessment of kidney tissue

TNF-α immunohistochemical staining sections of kidney tissues observed that intoxicated rats exposed to DZN (G4) showed strongly positive cytoplasmic reaction of the glomerular epithelial cells (Figure 6D). While intoxicated rats treated with NAC (G5) showed minimal positive cytoplasmic reactions of the glomerular epithelial cells (Figure 6E). TNF-α immunohistochemical staining sections of kidney tissues of normal control, olive oil, and NAC-treated rats showed a minimal reaction in the glomerular epithelial cells (Figure 6A, B, and C).

Morphometric study

The mean area percentage of Masson's Trichrome, and TNF-α immuno-expression for all groups are presented in Figures 5F, and 6F; respectively. The intoxicated rats treated with DZN (G4) showed a significant increase in the mean area percentage compared to normal control, olive oil, and NAC-treated rats. While intoxicated rats treated with NAC (G5) showed significant decrease in the mean area percentage.

DISCUSSION

DZN is an organophosphate insecticide that has a lot of commercial and agricultural uses. It is also one of the most common causes of poisoning, therefore its effect on various organs is important. DZN toxicity can be acute or chronic. Acute toxicity occurs in suicide or accidental ingestion, while chronic toxicity is due to long-term exposure (Yurumez *et al*., 2007). Upon entry into the body, DZN is metabolized by the cytochrome P 450 enzymes, which are present in most tissues of the body particularly in the liver, to highly toxic oxon intermediate metabolites. Several studies indicate that these oxon reactive metabolites cause tissue lipid peroxidation and oxidative stress. Lipids are one of the most susceptible biological molecules to ROS due to their interaction with other molecules to build cellular and organellar membranes (El-Demerdash and Nasr, 2014).

The kidney is responsible for elimination of active metabolites. DZN metabolites are excreted via kidney. However, DZN and its metabolites elimination through kidney are associated with kidney and tubular damage. Our study indicated that DZN has induced oxidative stress (manifested by significant decreases in CAT, SOD, GPx, and GSH, as well as a significant increase in MDA when compared with control) and kidney dysfunction that indicated by increases in serum creatinine and urea. Concentration of creatinine is a marker of kidney function, and its elevation is associated with kidney injury. Serum creatinine also shows kidney clearance. Therefore, increasing urea and creatinine is resulting from DZN-induced kidney damage and clearance reduction.

Indeed, the present results confirm that, like other OP insecticides, diazinon also has strongly oxidative properties even after sub-lethal exposures, as was evidenced by the raised MDA concentrations. A similar effect on LPO has been observed with other OP pesticides as well as diazinon (Durmaz *et al*., 2006), with a recent study reporting that Wistar rats orally treated with 10 mg/kg of diazinon showed significantly increased MDA in different tissues after 1, 4, and 7 weeks of treatment, the cause being either LPO induction or an increase in reactive oxygen species (Ogutcu *et al*., 2006). The increase in this marker in different tissues has been associated with oxidative stress, which is an imbalance between the generation of ROS and the antioxidant defense system. This imbalance favors the production of ROS rather than the antioxidant system, reducing the in vivo antioxidant capacity in the kidney, lungs, and liver (Ajibade *et al*., 2016). In the present study similar to previous investigations, MDA levels of kidney (Karimani *et al*., 2018) increased following DZN administration that is indicator of free radical formation of DZN in renal tissues.

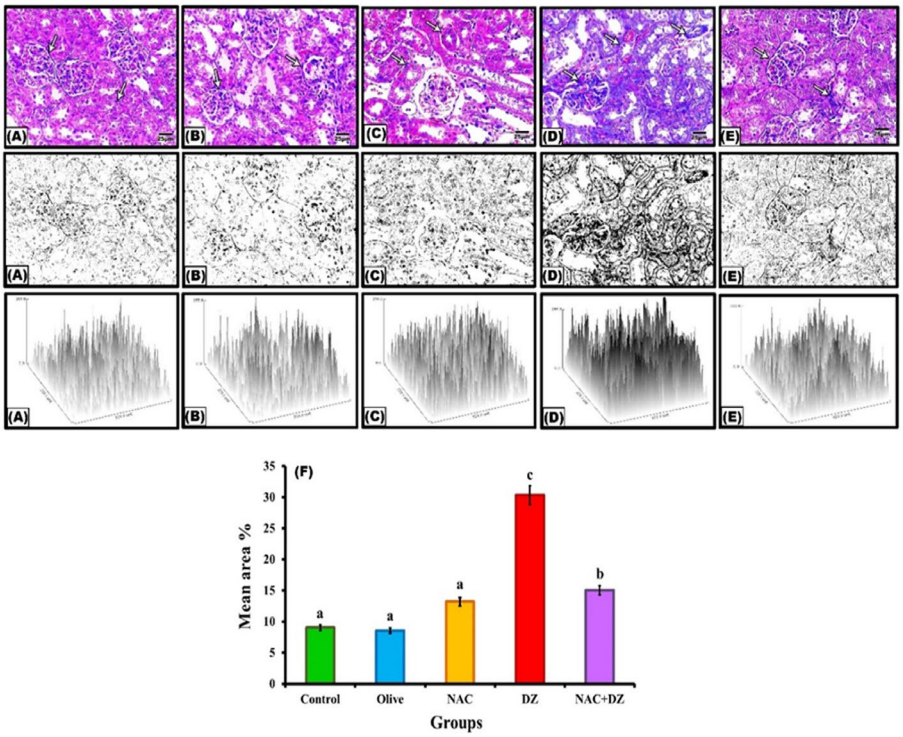

Fig. 5. Photomicrographs of kidney sections stained with Masson's trichrome; (A), (B), and (C) Normal control rat (G1), Olive oil treated rats (G2) and rat treated with N-Acetyl-Cysteine (NAC) (G3), the kidney showed minimal collagen fibers among the glomerular capillaries (arrow) and surrounding the renal corpuscles and tubules (arrow). (D) Intoxicated rats (G4) induced by diazinon; the kidney showed accumulation of collagen fibers among the glomerular capillaries (arrow) and surrounding the renal corpuscles and tubules (arrow). (E) Intoxicated rat by diazinon then treated with NAC (G5), showed minimal collagen fiber among the glomerular capillaries (arrow). (F) Histogram represents the mean area percentage of collagen fiber deposition in all experimental groups. (Scale bar represents 25 μm).

Additionally, reductions in antioxidant activities induced by DZN, our study provides further evidence that DZN can weaken tissue defences against oxidative stress damage by producing an excessive amount of ROS and depleting antioxidant power. Overall, it can be concluded that oxidative deterioration of the cell architecture, which may eventually result in cell death, is caused by peroxidation of membrane lipids due to redox imbalance under DZN-induced unfavourable conditions, particularly the O2-sensetive membrane-associated polyunsaturated fatty acids (Mossa *et al*., 2012; Karimani *et al*., 2018). Therefore, abnormal renal function determinants, as observed in DZN-treated rat, confirmed an indication of kidney damage (Karimani *et al*., 2019). These results were supported by histopathological and immunohistochemical examination of renal tissues which revealed dilated Bowman's space, inflammatory cell infiltration, glomerular and peritubular vascular congestion and swelling of renal tubular epithelium cells in DZN intoxicated group.

In the present work, increased consumption of GSH (as one of intracellular antioxidant defense system) in response to the sub-lethal diazinon exposure probably caused the general decrease in this biomarker's levels, similar to what other studies have observed in different organs of rats and mice in which GSH levels were identified as being clearly depressed (Hernández-Moreno *et al*., 2018). The depletion of GSH may be due to its increased use by cells to scavenge the free radicals produced by the pesticide, thus indicating the protective importance of this tripeptide to cope with oxidative substances (Leong *et al*., 2013). Because GSH can directly interact with and detoxify peroxynitrite (Knight *et al*., 2002) and is a co-substrate for glutathione peroxidase to reduce hydrogen peroxide (Brigelius-Flohé and Flohé, 2020).

Catalase is the predominant enzyme in regulating and controlling intracellular H2O2 concentrations, being involved in the second line of defense against ROS (Ajibade *et al*., 2016). Several previous results confirm the effect of diazinon weakening the animals' enzymatic antioxidant defense system (Abbasnezhad *et al*., 2009).

The relationship between cellular senescence and fibrosis can be explained by the pro-inflammatory microenvironment produced by senescent cells. Senescent cells express a range of secreted factors consisting of various proinflammatory molecules, metalloproteases, and growth factors. This phenomenon is termed as senescence-associated secretory phenotype (SASP), which affects tissue and organ function (Van Deursen, 2014; Childs *et al*., 2015). In the present study, we detected increased serum levels of proinflammatory factors including IL-1β, TNF-α, as well as renal tissue TNF-α immune-expression besides the mRNA expression and protein levels of pro-apoptotic factor BAX and decreased mRNA expression and protein levels in renal tissue of anti-apoptotic factor BCL2 of rats-treated with DZN. Components of the SASP attract and activate immune cells to destroy the tissue environment. In addition, SASP components including IL-6 can stimulate fibrosis of specific epithelial tissues by inducing epithelial mesenchymal transition (EMT) (Van Deursen, 2014). Hence, senescence-mediated extracellular matrix remodeling through the SASP is a potential mechanism underlying premature senescence-associated fibrosis in renal tissue of DZN treated rats. These results were confirmed in the current study by increased collagen area percentage in DZN group.

N-acetylcysteine (NAC), a thiol donor compound, is a precursor to various antioxidants in the human body (Samuni *et al*., 2013). NAC has a variety of biological functions, mainly involved in the decomposition of peroxides in the body and the storage of cellular glutathione (Zafarullah *et al*., 2003). NAC exhibits direct and indirect antioxidant properties. NAC interacts with hydrogen peroxide and hypochlorous acid, by its free thiol group that serves as an electron donor (Aruoma *et al*., 1989). This interaction leads to intermediate formation of NAC thiol, with NAC disulphide as a major end product. Further, NAC has indirect antioxidant propriety related to its role as a GSH precursor. Its main property to increase the level of GSH was proven by several studies in vitro and in vivo (Lasram *et al*., 2015). This powerful ability of NAC to control oxidative stress and to increase GSH synthesis may play an important role in the protection of renal cell s against damage induced by DZN. In this context, our histopathological results revealed near normal histological structure as there were decreased of Bowman's space dilatation, inflammatory cell infil-

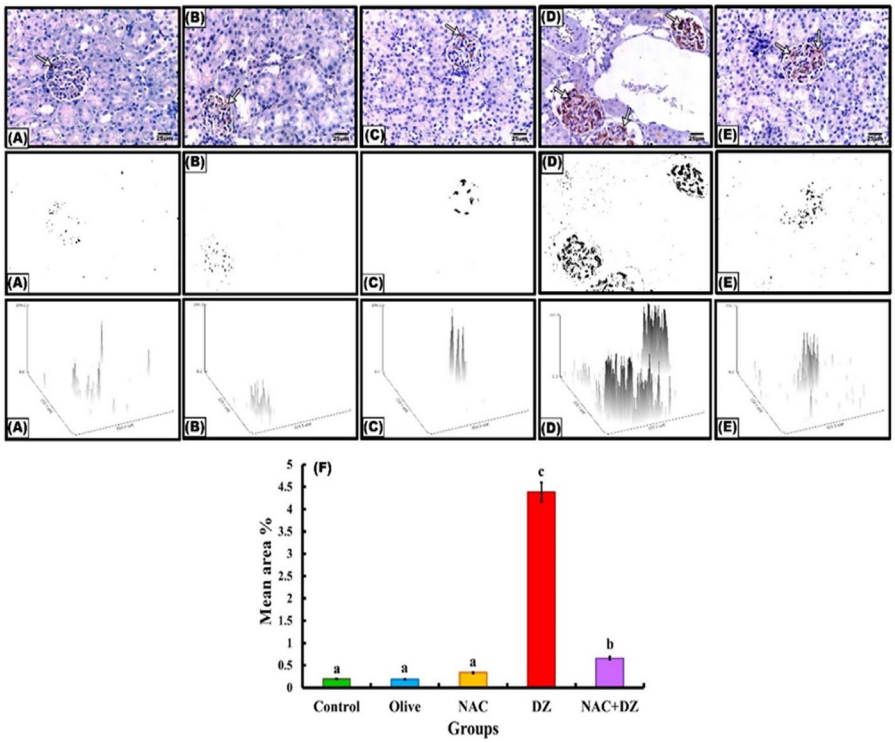

Fig. 6. Tumor necrosis factor alpha (TNF-α) immunohistochemical staining sections of kidney of experimental rats. (A), (B), and (C) Normal control rats (G1), Olive oil treated rats (G2) and rats treated with N-Acetyl-Cysteine (NAC) (G3), showed minimal reaction in the glomerular epithelial cells. (D) Intoxicated rats (G4) induced by diazinon; showed strong positive cytoplasmic reaction in glomerular epithelial cells (arrow). (E) Intoxicated rat by diazinon then treated with NAC (G5), showed minimal positive cytoplasmic reaction in the glomerular epithelial cells (arrow). (F) Histogram representing the mean area percentage of TNF-α immunoreaction in all experimental groups. (Anti-TNF-α, ×400) (Scale bar represents 25 μm).

tration, reduction of glomerular and peritubular vascular congestion and reduction of the renal tubular epithelium cells swelling.

In addition to causing oxidative damage, ROS induced by DZN toxicity activates inflammatory pathways, and as a result, they trigger the expression of inflammatory proteins which are confirmed by increased serum concentrations of IL-1β and TNF-α. TNF-α, IL-1β as well as increased TNFα immune-expression and other cytokines exert paracrine effects to activate inflammatory pathways in insulin target cells. This leads to the activation of Jun N-terminal kinase (JNK), inhibitor of κB kinase (IKKβ), and other serine kinases (Lasram *et al*., 2015). The anti-inflammatory properties of NAC have been reported by various studies. Indeed, it was reported that NAC limits cytokine release during the initial phase of immune proliferation (Omara *et al*., 1997). Similarly, another study has highlighted a decrease in TNF-α in septic shock by administering NAC (Emet *et al*., 2004). Furthermore, NAC reduces the production of IL-6 in hemodialysis patients (Nascimento *et al*., 2010) and decreases the levels of proinflammatory cytokines TNFα and IL-1β in rodents subjected to focal cerebral ischemia (Khan *et al*., 2004; Chen *et al*., 2008). The anti-inflammatory effects of NAC were associated to the decrease of NF-κB activity. NF-κB is naturally bound to I-κB that prevents its nuclear translocation. Dissociation of I-κB following its phosphorylation by IKKβ allows its degradation by the proteasome, and the transport of NF-κB to the nucleus. NAC suppressed the proteasome activity, thereby inhibiting NF-κB activation (Pajonk *et al*., 2002). Furthermore, NAC also inhibited the IKK themselves (Oka *et al*., 2000). Indeed, NF-κB has been shown to be activated in the absence of I-κB degradation through an iron-mediated mechanism (Jimenez *et al*., 2000). On the other hand, NAC can modulate the expression and the activity of transcription factors (Samuni *et al*., 2013). This raises the possibility that NAC promotes the synthesis of certain proteins which inhibit the activation of IKKβ/NF-κB axis. The effects of NAC may be dependent on the synthesis of glutathione, suggesting that the inhibition of NF-κB by the suppression of IKKβ could be the result of the indirect action of NAC. However, this does not necessarily exclude the role of free radicals in the modulation of NF-κB activity. As a direct consequence of its antioxidant properties, NAC allows maintaining the cellular redox state, and thus can modulate the activity of redox-sensitive transcription factors such as NF-κB (Zafarullah *et al*., 2003).

NAC has, at the same time, antiapoptotic and cell growth stimulatory properties. As related by Aksoy *et al*. (2010). NAC can have different effects on apoptosis. Many data reported the ability of NAC to inhibit apoptosis while minor other showed no effect of NAC and a few showed an increase of apoptosis by NAC administration. Nevertheless, it has been demonstrated that NAC blocks apoptosis induced by LPS in endothelial cells (Abello *et al*., 1994), and apoptosis induced by TNF-α in neuronal cells (Talley *et al*., 1995). Moreover, NAC inhibits cytotoxic and apoptotic effects of certain compounds such as paraquat (Hong *et al*., 2003), cadmium (Abe *et al*., 1998) and cisplatin (Cui-E *et al*., 2005). Moreover, it was reported that NAC suppresses the ROS production and apoptotic cell death in C6 cells (Sun *et al*., 2012) and protects against monosodium glutamate-induced astrocytic cell death (Park *et al*., 2014). In contrast, at high concentrations NAC appears to have cytotoxic effects that are cell-specific (Kawada *et al*., 1998).

The present study has revealed that exposure to subchronic doses of DZN impairs the kidney structure and function, as evidenced by the histopathology, immunohistochemistry, and gene expression of NLRP3, NFκB, IKB, BCL2, BAX mRNA. However, NAC has shown to play a beneficial role against nephrotoxicity by reversing the cytoarchitecture and downregulation of inflammatory (NLRP3, NFκB, IKB) and apoptotic (BAX) as well as upregulated BCL2 genes in kidney tissues, bringing them to near-normal levels. These effects could be attributed to the antioxidant and anti-inflammatory properties of NAC. Therefore, NAC could be potentially used to protect the kidneys from pathological changes induced by DZN.

CONCLUSION

As a potential nephroprotective drug against DZN-induced nephrotoxicity, NAC was highlighted in the current investigation. As NAC enhanced kidney CAT, SOD, GPx, and GSH antioxidant levels as well as inhibited the production of TNF-α in renal tissues, it protected the kidney from the DZN insult and decreased lipid peroxidation through lowering kidney MDA levels. NAC's ability to combat oxidative stress may be related to its modification of the NLRP3, NFκB, and IKB pathway and the subsequent overexpression of antioxidant enzymes like CAT, SOD, GPx, and GSH. Therefore, this research might help NAC be used in the future as a nephroprotective drug, increasing its medical usefulness.

CONFLICT OF INTEREST

The authors declare that they have no competing interests.

REFERENCES

Abbasnezhad, M., Jafari, M., HagHooseni, R., Haggholamali, M., Salehi, M., Salimian, M., 2009. Acute toxicity effect of paraoxon on kidney lipid peroxidation and antioxidant system. Toxicology Letters 189, S125-S125.

Abe, T., Yamamura, K., Gotoh, S., Kashimura, M., Higashi, K., 1998. Concentration-dependent differential effects of N-acetyl-L-cysteine on the expression of HSP70 and metallothionein genes induced by cadmium in human amniotic cells. Biochimica et Biophysica Acta (BBA)-General Subjects 1380, 123-132.

Abello, P.A., Fidler, S.A., Bulkley, G.B., Buchman, T.G., 1994. Antioxidants modulate induction of programmed endothelial cell death (apoptosis) by endotoxin. Archives of Surgery 129, 134-141.

Ajibade, T.O., Oyagbemi, A.A., Omobowale, T.O., Asenuga, E.R., Afolabi, J.M., Adedapo, A.A., 2016. Mitigation of diazinon-induced cardiovascular and renal dysfunction by gallic acid. Interdisciplinary toxicology 9, 66-77.

Aksoy, Y., Kesik, K., Canpinar, H., 2010. Does N-Acetyl Cysteine Protect Against Apoptosis in HL60 Cell Line?. Turkish Journal of Biochemistry 35, 333-339.

Aldini, G., Altomare, A., Baron, G., Vistoli, G., Carini, M., Borsani, L., Sergio, F., 2018. N-Acetylcysteine as an antioxidant and disulphide breaking agent: the reasons why. Free Radical Research 52, 751-762.

Aruoma, O.I., Halliwell, B., Hoey, B.M., Butler, J., 1989. The antioxidant action of N-acetylcysteine: its reaction with hydrogen peroxide, hydroxyl radical, superoxide, and hypochlorous acid. Free Radical Biology and Medicine 6, 593-597.

Bradford, M.M., 1976. A rapid and sensitive method for the quantitation of microgram quantities of protein utilizing the principle of protein-dye binding. Analytical Biochemistry 72, 248-254.

Brigelius-Flohé, R., Flohé, L., 2020. Regulatory phenomena in the glutathione peroxidase superfamily. Antioxidants and Redox Signaling 33, 498-516.

Chen, G., Shi, J., Hu, Z., Hang, C., 2008. Inhibitory effect on cerebral inflammatory response following traumatic brain injury in rats: a potential neuroprotective mechanism of N-acetylcysteine. Mediators of Inflammation 2008, 716458.

Childs, B.G., Durik, M., Baker, D.J., Van Deursen, J.M., 2015. Cellular senescence in aging and age-related disease: from mechanisms to therapy. Nature Medicine 21, 1424-1435.

Cui-E, W., Yan-Lin, Y., Dong-Xing, J., Tao, Z., Hui, H., Zhi-Huan, L., Xiang-Qing, L., Zhi-Qiang, C., Qing-Yuan, H., Gao-Long, Z., 2005. The Reaction Cross Section and Neutron Removal Cross Sections of 17C. Chinese Physics C 29, 1052-1056.

Danaei, G.H., Memar, B., Ataee, R., Karami, M., 2019. Protective effect of thymoquinone, the main component of Nigella Sativa, against diazinon cardio-toxicity in rats. Drug and Chemical Toxicology 42, 585-591.

Durmaz, H., Sevgiler, Y., Üner, N., 2006. Tissue-specific antioxidative and neurotoxic responses to diazinon in Oreochromis niloticus. Pesticide Biochemistry and physiology 84, 215-226.

Eddleston, M., Karalliedde, L., Buckley, N., Fernando, R., Hutchinson, G., Isbister, G., Konradsen, F., Murray, D., Piola, J.C., Senanayake, N., 2002. Pesticide poisoning in the developing world—a minimum pesticides list. The Lancet 360, 1163-1167.

El-Demerdash, F.M., Nasr, H.M., 2014. Antioxidant effect of selenium on lipid peroxidation, hyperlipidemia and biochemical parameters in

rats exposed to diazinon. Journal of Trace Elements in Medicine and Biology 28, 89-93.
Emet, S., Memis, D., Pamukçu, Z., 2004. The influence of N-acetyl cysteine infusion oncytokine levels and gastric intramucosal pH during severe sepsis. Critical Care 8, R172-9.
Hamad, M.H., Adeel, A.A., Alhaboob, A.A.N., Ashri, A.M., Salih, M.A., 2016. Acute poisoning in a child following topical treatment of head lice (*Pediculosis capitis*) with an organophosphate pesticide. Sudanese journal of paediatrics 16, 63.
Hegazy, A.M., Hafez, A.S., Eid, R.M., 2020. Protective and antioxidant effects of copper-nicotinate complex against glycerol-induced nephrotoxicity in rats. Drug and Chemical Toxicology 43, 234–239.
Hernández-Moreno, D., Míguez, M.P., Soler, F., Pérez-López, M., 2018. Influence of sex on biomarkers of oxidative stress in the kidney, lungs, and liver of rabbits after exposure to diazinon. Environmental Science and Pollution Research 25, 32458-32465.
Hong, S.Y., Yang, J.O., Lee, E.Y., Lee, Z.W., 2003. Effects of N-acetyl-L-cysteine and glutathione on antioxidant status of human serum and 3T3 fibroblasts. Journal of Korean Medical Science 18, 649-654.
Jimenez, L., Thompson, J., Brown, D., Rahman, I., Antonicelli, F., Duffin, R., Drost, E., Hay, R., Donaldson, K., MacNee, W., 2000. Activation of NF-κB by PM10 occurs via an iron-mediated mechanism in the absence of IκB degradation. Toxicology and Applied Pharmacology 166, 101-110.
Joshi, D., Mittal, D.K., Shukla, S., Srivastav, A.K., Srivastav, S.K., 2014. N-acetyl cysteine and selenium protects mercuric chloride-induced oxidative stress and antioxidant defense system in liver and kidney of rats: a histopathological approach. Journal of Trace Elements in Medicine and Biology 28, 218-226.
Karimani, A., Heidarpour, M., Moghaddam Jafari, A., 2019. Protective effects of glycyrrhizin on sub-chronic diazinon-induced biochemical, hematological alterations and oxidative stress indices in male Wistar rats. Drug and Chemical Toxicology 42, 300-308.
Karimani, A., Mamashkhani, Y., Jafari, A.M., Akbarabadi, M., Heidarpour, M., 2018. Captopril attenuates diazinon-induced oxidative stress: a subchronic study in rats. Iranian journal of Medical Sciences 43, 514.
Kawada, N., Seki, S., Inoue, M., Kuroki, T., 1998. Effect of antioxidants, resveratrol, quercetin, and N-acetylcysteine, on the functions of cultured rat hepatic stellate cells and Kupffer cells. Hepatology 27, 1265-1274.
Khan, M., Sekhon, B., Jatana, M., Giri, S., Gilg, A.G., Sekhon, C., Singh, I., Singh, A.K., 2004. Administration of N-acetylcysteine after focal cerebral ischemia protects brain and reduces inflammation in a rat model of experimental stroke. Journal of Neuroscience Research 76, 519-527.
Knight, T.R., Ho, Y.-S., Farhood, A., Jaeschke, H., 2002. Peroxynitrite is a critical mediator of acetaminophen hepatotoxicity in murine livers: protection by glutathione. Journal of Pharmacology and Experimental Therapeutics 303, 468-475.
Lasram, M.M., Dhouib, I.B., Annabi, A., El Fazaa, S., Gharbi, N., 2015. A review on the possible molecular mechanism of action of N-acetylcysteine against insulin resistance and type-2 diabetes development. Clinical biochemistry 48, 1200-1208.
Leong, C.T., D'Souza, U.J., Iqbal, M., Mustapha, Z.A., 2013. Lipid peroxidation and decline in antioxidant status as one of the toxicity measures of diazinon in the testis. Redox report 18, 155-164.
Livak, K.J., Schmittgen, T.D., 2001. Analysis of relative gene expression data using real-time quantitative PCR and the $2^{-\Delta\Delta CT}$ method. Methods 25, 402-408.
Millea, P.J., 2009. N-acetylcysteine: multiple clinical applications. American Family Physician 80, 265-269.
Mokhtari, V., Afsharian, P., Shahhoseini, M., Kalantar, S.M., Moini, A., 2017. A review on various uses of N-acetyl cysteine. Cell Journal (Yakhteh) 19, 11.
Mossa, A.-T.H., Heikal, T.M., Omara, E.A.A., 2012. Physiological and histopathological changes in the liver of male rats exposed to paracetamol and diazinon. Asian pacific Journal of Tropical Biomedicine 2, S1683-S1690.
Nascimento, M.M., Suliman, M.E., Silva, M., Chinaglia, T., Marchioro, J., Hayashi, S.Y., Riella, M.C., Lindholm, B., Anderstam, B., 2010. Effect of oral N-acetylcysteine treatment on plasma inflammatory and oxidative stress markers in peritoneal dialysis patients: a placebo-controlled study. Peritoneal dialysis international 30, 336-342.
Ogutcu, A., Uzunhisarcikli, M., Kalender, S., Durak, D., Bayrakdar, F., Kalender, Y., 2006. The effects of organophosphate insecticide diazinon on malondialdehyde levels and myocardial cells in rat heart tissue and protective role of vitamin E. Pesticide Biochemistry and Physiology 86, 93-98.
Oka, S.-i., Kamata, H., Kamata, K., Yagisawa, H., Hirata, H., 2000. N-Acetylcysteine suppresses TNF-induced NF-κB activation through inhibition of IκB kinases. FEBS letters 472, 196-202.
Oksay, T., Nazıroğlu, M., Ergün, O., Doğan, S., Özatik, O., Armağan, A., Özorak, A., Çelik, Ö.J.A., 2013. N-acetyl cysteine attenuates diazinon exposure-induced oxidative stress in rat testis. Andrologia 45, 171-177.
Omara, F.O., Blakley, B.R., Bernier, J., Fournier, M., 1997. Immunomodulatory and protective effects of N-acetylcysteine in mitogen-activated murine splenocytes in vitro. Toxicology 116, 219-226.
Owumi, S., Bello, T., Oyelere, A.K., 2021. N-acetyl cysteine abates hepatorenal toxicities induced by perfluorooctanoic acid exposure in male rats. Environmental Toxicology and Pharmacology 86, 103667.
Pajonk, F., Riess, K., Sommer, A., McBride, W.H., 2002. N-acetyl-L-cysteine inhibits 26S proteasome function: implications for effects on NF-κB activation. Free Radical Biology and Medicine 32, 536-543.
Park, E., Yu, K.H., Kim, D.K., Kim, S., Sapkota, K., Kim, S.-J., Kim, C.S., Chun, H.S., 2014. Protective effects of N-acetylcysteine against monosodium glutamate-induced astrocytic cell death. Food and Chemical Toxicology 67, 1-9.
Pathak, V.M., Verma, V.K., Rawat, B.S., Kaur, B., Babu, N., Sharma, A., Dewali, S., Yadav, M., Kumari, R., Singh, S., 2022. Current status of pesticide effects on environment, human health and it's eco-friendly management as bioremediation: A comprehensive review. Frontiers in Microbiology 13, 2833.
Rashedinia, M., Hosseinzadeh, H., Imenshahidi, M., Lari, P., Razavi, B.M., Abnous, K.J.T., Health, I., 2016. Effect of exposure to diazinon on adult rat's brain. Toxicol Ind Health 32, 714-720.
Samuni, Y., Goldstein, S., Dean, O.M., Berk, M., 2013. The chemistry and biological activities of N-acetylcysteine. Biochimica et Biophysica Acta (BBA)-General Subjects 1830, 4117-4129.
Skeggs, L.T., 1957. An automatic method for colorimetric analysis. American Journal of Clinical Pathology 28, 311-322.
Smith, A., Yu, X., Yin, L., 2018. Diazinon exposure activated transcriptional factors CCAAT-enhancer-binding proteins α (C/EBPα) and peroxisome proliferator-activated receptor γ (PPARγ) and induced adipogenesis in 3T3-L1 preadipocytes. Pesticide Biochemistry and Physiology 150, 48-58.
Sun, L., Gu, L., Wang, S., Yuan, J., Yang, H., Zhu, J., Zhang, H., 2012. N-acetylcysteine protects against apoptosis through modulation of group I metabotropic glutamate receptor activity. PLoS One 7, e32503.
Suvarna, K., Layton, C., Bancroft, J., 2019. Pigments and minerals. Bancroft's Theory and Practice of Histological Techniques, Eighth edn: ELSEVIER, p. 166.
Suvarna, K.S., Layton, C., Bancroft, J., 2013. Immunohistochemical techniques. Bancroft's Theory and Practice of Histological Techniques. 7th ed., Churchill Livingstone, Philadelphia, pp. 381-426.
Talley, A.K., Dewhurst, S., Perry, S.W., Dollard, S.C., Gummuluru, S., Fine, S.M., New, D., Epstein, L.G., Gendelman, H.E., Gelbard, H.A., 1995. Tumor necrosis factor alpha-induced apoptosis in human neuronal cells: protection by the antioxidant N-acetylcysteine and the genes Bcl2 and crmA. Molecular and Cellular Biology 15, 2359-2366.
Van Deursen, J.M., 2014. The role of senescent cells in ageing. Nature 509, 439-446.
Weissman, M., Pileggi, V., Henry, R., Cannon, D., Winkelman, J., 1974. Clinical chemistry: principles and techniques, Harper and Row Publishers, Hagerstown, MD.
Yurumez, Y., Durukan, P., Yavuz, Y., Ikizceli, I., Avsarogullari, L., Ozkan, S., Akdur, O., Ozdemir, C., 2007. Acute organophosphate poisoning in university hospital emergency room patients. Internal Medicine 46, 965-969.
Zafarullah, M., Li, W., Sylvester, J., Ahmad, M., 2003. Molecular mechanisms of N-acetylcysteine actions. Cellular and Molecular Life Sciences CMLS 60, 6-20.